# Selective mode excitation and discrimination of four-core homogeneous coupled multi-core fiber

**Yasuo Kokubun,[1,*] Toshinori Komo,[1] Katsuhiro Takenaga,[2] Shoji Tanigawa,[2] and Shoichiro Matsuo[2]**

[1] *Graduate School of Eng., Yokohama National University, 79-5 Tokiwadai, Hodogaya-ku, Yokohama, 240-8501, Japan*

[2] *Optics and Electronics Laboratory, Fujikura Ltd., 1440 Matsuzaki, Sakura, Chiba, 285-8550, Japan*

*ykokubun@ynu.ac.jp

**Abstract:** Coupled modes of homogeneous coupled multi-core fiber are selectively excited and discriminated utilizing the difference of equivalent propagation angle. To quantatively evaluate the extinction ratio (selectivity) of adjacent modes, a new mode discrimination technique is developed by measuring the visibility of far-field patterns under small change of wavelength of the launching beam. The peak angles of discriminated far-field patterns show a strong correlation with the incident angle of the launching beam, which means that the coupled modes were selectively excited and discriminated.



**OCIS codes:** (060.2270) Fiber characterization; (060.2280) Fiber design and fabrication.

## References and links

1. M. Koshiba, K. Saitoh, and Y. Kokubun, "Heterogeneous multi-core fibers: Proposal and design principle," IEICE Electron. Express **6**, 98–103 (2009).
2. Y. Kokubun and M. Koshiba, "Novel multi-core fibers for mode division multiplexing: Proposal and design principle," IEICE Electron. Express **6**, 522–528 (2009).
3. X. Liu, S. Chandrasekhar, X. Chen, P. Winzer, Y. Pan, B. Zhu, T. Taunay, M. Fishteyn, M. Yan, J. M. Fini, E. Monberg, and F. Dimarcello, "1.12-TB/S 32-QAM-OFDM Superchannel with 8.6-B/s/Hz Intrachannel Spectral Efficiency and Space-Division Multiplexing with 60-B/s/Hz Aggregate Spectral Efficiency," in *Proceedings of 37th European Conference on Optical Communication*, (Geneva, Switzerland, 2011), paper Th.13.B.1.
4. R. Ryf, A. Sierra, R-J. Essiambre, A. Gnauck, S. Randel, M. Esmaeelpour, S. Mumtaz, P. Winzer, R. Delbue, P. Pupalaikis, A. Sureka, T. Hayashi, T. Taru, and T. Sasaki, "Coherent 1200km 6x6 MIMO Mode-Multiplexed Transmission over 3-Core Microstructured Fiber," in *Proceedings of 37th European Conference on Optical Communication*, (Geneva, Switzerland, 2011) paper Th.13.C.1.
5. B. Zhu, T. F. Taunay, M. F. Yan, J. M. Fini, M. Fishteyn, E. M. Monberg, and F. V. Dimarcello, "Seven-core multicore fiber transmissions for passive optical network," Opt. Express **18**, 11117–11122 (2010).
6. J. M. Fini, T. Taunay, B. Zhu, and M. Yan, "Low cross-talk design of multi-core fibers," in *Proceedings of Conference on Lasers and Electro-Optics/Quantum Electronics and Laser Science*, (San Jose, CA, 2011), paper CTuAA3.
7. K. Imamura, K. Mukasa, and T. Yagi, "Investigation on Multi-Core Fibers with Large Aeff and Low Micro Bending Loss," in *Proceedings of Optical Fiber Communications Conference*, (San Diego, CA, 2010), paper OWK6.
8. K. Takenaga, S. Tanigawa, N. Guan, S. Matsuo, K. Saito, and M. Koshiba, "Reduction of Crosstalk by Quasi-Homogeneous Solid Multi-Core Fiber," in *Proceedings of Optical Fiber Communications Conference*, (San Diego, CA, 2010), paper OWK7.

#155638 - $15.00 USD Received 29 Sep 2011; revised 21 Nov 2011; accepted 23 Nov 2011; published 8 Dec 2011

9. J. M. Fini, B. Zhu, T. F. Taunay, and M. F. Yan, "Statistics of crosstalk in bent multicore fibers," Opt. Express **18**, 15122–15129 (2010).
10. T. Hayashi, T. Taru, O. Shimakawa, T. Sasaki, and E. Sasaoka, "Low-Crosstalk and Low-Loss Multi-Core Fiber Utilizing Fiber Bend," in *Proceedings of Optical Fiber Communications Conference*, (Los Angeles, CA, 2011), paper OWJ3.
11. K. Takenaga, Y. Arakawa, S. Tanigawa, N.Guan, S. Matsuo, K. Saito, M. Koshiba, "Reduction of Crosstalk by Trench-Assisted Multi-Core Fiber,hin *Proceedings of Optical Fiber Communications Conference*, (Los Angeles, CA, 2011), paper OWJ4.
12. K. Tomozawa and Y. Kokubun, "Maximum core capacity of heterogeneous uncoupled multi-core fibers," in *Proceedings of 15th Optoelectronics and Communications Conference*, (Sapporo, Japan, 2010), paper 7C2-4.
13. H. Haus and L. Molter-Orr, "Coupled multiple waveguide systems," IEEE J. Quantum Electron. **QE-19**, 840–844 (1983).

## 1. Introduction

Heterogeneous uncoupled multi-core fiber (MCF) [1] and homogeneous coupled MCF [2] were proposed as means to greatly enhance the transmission capacity of optical fibers using space division multiplexing and mode division multiplexing, and recently ultra-high capacity and long distance transmission experiments have been demonstrated using a seven core uncoupled multi-core fiber [3] and 3-core microstructured fiber [4]. Despite theoretical and experimental research [5 – 11] of the crosstalk and bending characteristics of seven-core heterogeneous uncoupled MCF's, these properties had not been investigated or researched for homogeneous uncoupled MCFfs because of the lack of necessary selective excitation of coupled modes and mode discrimination. When high $\Delta$ cores with 5 $\mu$m diameter ( $\Delta = 1.1 - 1.4\%$ ) is used, 78 cores can be accommodated in a 125 $\mu$m diameter fiber using a hybrid arrangement of homogeneous coupled MCF [2], while 55 cores can be accommodated using the heterogeneous uncoupled MCF with nine types of non-identical cores [12]. Since the core density of homogeneous coupled MCF can be higher than that of heterogeneous uncoupled MCF by applying a hybrid core arrangement [2], further development of MCF's requires a clearer understanding of the crosstalk of homogeneous coupled multi-core fibers.

In this paper, we propose and demonstrate exciting selected coupled modes guided in a four-core homogeneous coupled MCF, applying the same principle as a mode multiplexer [2]. Using the differences between propagation angles of coupled modes, each coupled mode was selectively excited by adjusting the incident angle of the launching beam to the propagation angle of the coupled mode. The excitation profile of coupled modes is observed using the near-field pattern and the far-field pattern (FFP), corresponding to the propagation angle. In the FFP measurements, we observed a small variation of FFP when the wavelength was slightly changed. This implies that a small amount of the adjacent mode is simultaneously excited and the interference between coupled modes with adjacent mode orders is observed. Therefore, we developed a new mode discrimination method by calculating the far-field patterns from the visibility measurements. As a result, the peak angles of coupled modes of discriminated FFP were in good agreement with the incident angles of the launching beam as well as the numerical results.

## 2. Design and fabrication of four-core homogeneous coupled multi-core fiber

The homogeneous coupled MCF designed and fabricated in this work consists of four single-mode cores as shown in Fig. 1, where the core radius $a$ and the relative index difference $\Delta$ are all the same. The operating wavelength is 1.55 $\mu$m.

Since the core distance $D$ is designed to be in close proximity ($D$=2$a$), four cores are strongly coupled and four coupled modes are created in a strongly coupled system. The propagation constant difference between coupled modes is increased with the decrease of core distance $D$ as shown in Fig. 2.

#155638 - $15.00 USD Received 29 Sep 2011; revised 21 Nov 2011; accepted 23 Nov 2011; published 8 Dec 2011

This difference of propagation constants and the orthogonality of coupled modes can be utilized as an independent transmission channel. There should be a large difference between propagation constants of coupled modes to prevent mode conversion caused by a small perturbations such as fine irregularities at core boundaries. To extend the difference of the propagation constant between adjacent coupled modes, the relative index difference $\Delta$ was designed to be 1.4 %. In this case, the difference of equivalent indices between the fundamental coupled mode and the first order coupled mode is about 60 % of the difference between the equivalent index of the fundamental mode and the cladding index for ordinary single mode fiber with $\Delta = 0.3$ %. This results in a sufficiently large difference of propagation constants between adjacent coupled modes.

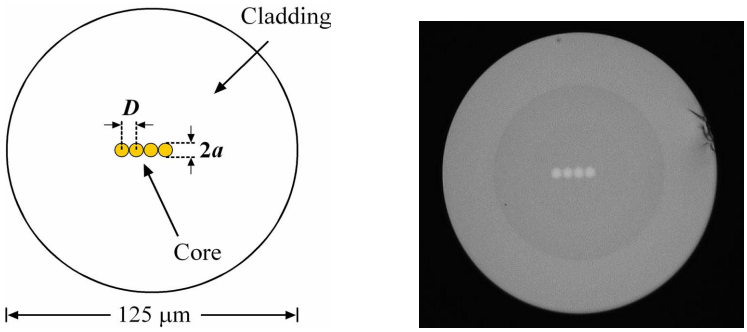


(a) Cross-sectional structure (b) Optical microscope image

Fig. 1. Structure and definition of parameters of four-core homogeneous coupled MCF.

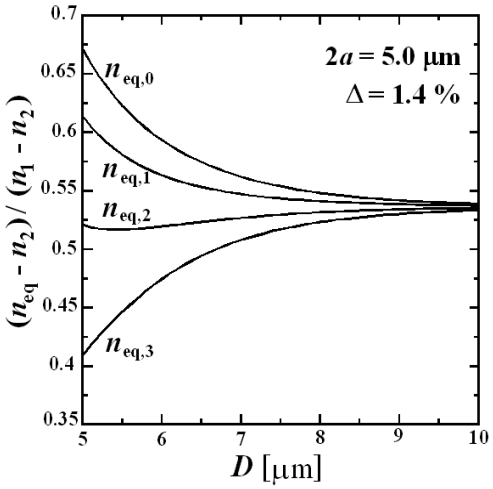


Fig. 2. Normalized equivalent index of coupled modes in homogeneous coupled MCF as a function core-to-core distance.

The core diameter 2$a$ was designed to be 5.0 $\mu$m to satisfy the single-mode condition. The cutoff wavelength of the single mode core used for this homogeneous MCF was measured to be 1.35 $\mu$m. The calculated equivalent indices of coupled modes that were calculated using a

#155638 - $15.00 USD Received 29 Sep 2011; revised 21 Nov 2011; accepted 23 Nov 2011; published 8 Dec 2011

Table 1. Calculated quivalent indices of coupled modes.

| | Fundamental mode | 1st order mode | 2nd order mode | 3rd order mode |
|---|---|---|---|---|
| $n_{eq}$ | 1.449465 | 1.448401 | 1.44673 | 1.444785 |

The refractive indices of core and cladding are $n_1 = 1.45886$ and $n_2 = 1.43824$, respectively.

mode solver (FemSIM by Rsoft Inc.) are summarized in Table 1. The mode field diameter of single core was calculated to be 7.7 $\mu$m.

## 3. Coupled mode excitation and discrimination

A mode multiplexer is required to launch a homogeneous coupled multi-core fiber while discriminating between each mode. This result can be achieved by modifying arrayed waveguide grating filter [2]. Since the phase difference of the field of $\nu$-th order coupled mode between adjacent cores in a multiple coupled waveguide is given by $\pm \frac{\nu}{N-1}\pi$ as shown in Fig. 3 [13], where $N$ is the number of coupled waveguides, the equivalent propagation angle corresponding to the normal direction of equivalent wavefront also depends on the mode order $\nu$ as well as the core diameter, core spacing and the wavelength. The principle of the mode multiplexer/demultiplexer is based on the difference of the propagation angles of coupled modes, and so the equivalent function can be realized by changing the incident angle of the launching beam at the beam waist as shown in Fig. 4. The wavelength of the launching beam was 1.55 $\mu$m, and the beam diameter was expanded to 20 $\mu$m to cover the width of the one-dimensional array of four cores (20 $\mu$m). The fiber length was 100m.

The theoretical coupling loss from the circular Gaussian beam with the beam diameter of 20 $\mu$m to the fundamental coupled mode was calculated to be 1.56 dB, and this loss can be improved by the use of cylindrical lens to adjust the aspect ratio of the incident beam to that of the coupled mode. In the practical optical fiber communication system, a waveguide-type mode multiplexer [2] will be required. As for the propagation loss, since the length of the tested fiber (100m) was not long enough to measure the propagation loss by the cut-back method, the propagation loss of longer fiber was measured using the OTDR (Optical Time Domain Reflectometry) method. However, the measured result was 11 dB/km. Since a single mode fiber was connected to one of four cores near the center and the reflected light was detected only from the single core, this result seems to differ from the actual propagation loss. The propagation loss of each coupled mode should be measured by this mode discrimination technique, and the measured result by the technique described in this paper using longer fiber than this tested fiber will be presented in future.

The coupled modes guided in the homogeneous MCF must be discriminated at the output end. First the near-field patterns were observed when the incident angle of the launching beam was adjusted to the propagation angle of each coupled mode. A near-field observation system consisting of microscope lens and InGaAs infrared imaging system (C10633-13 by Hamamatsu Photonics Inc.) was used for the NFP measurement. The image size is $320\times256$ pixels, and the dynamic range of intensity digitization is 14 bits. The observed NFP's are shown in Fig. 5 and the calculated NFP's are shown in Fig. 6 for comparison. In addition, the calculated field amplitude patterns are shown in Fig. 7 for comparison with Fig. 3 The incident angles of the launching beam are summarized in Table 2. It is seen from Fig. 5 and Fig. 6 that the observed NFP of each coupled mode coincidents well with the theoretical intensity pattern that were calculated using a mode solver (FemSIM by Rsoft Inc.).

Next, we observed the far-field patterns for incident angles of the launching beam corresponding to the propagation angle of coupled modes. Since the far-field observation can dis-

#155638 - $15.00 USD Received 29 Sep 2011; revised 21 Nov 2011; accepted 23 Nov 2011; published 8 Dec 2011

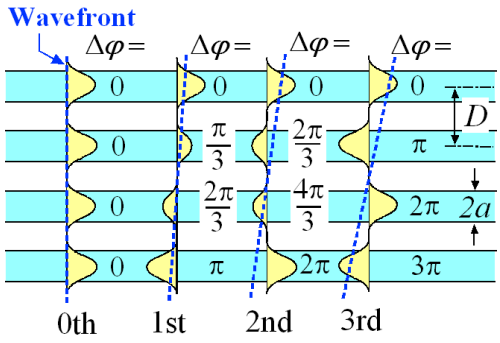


Fig. 3. Field profiles and phase profiles of coupled modes in a four-coupled waveguide.

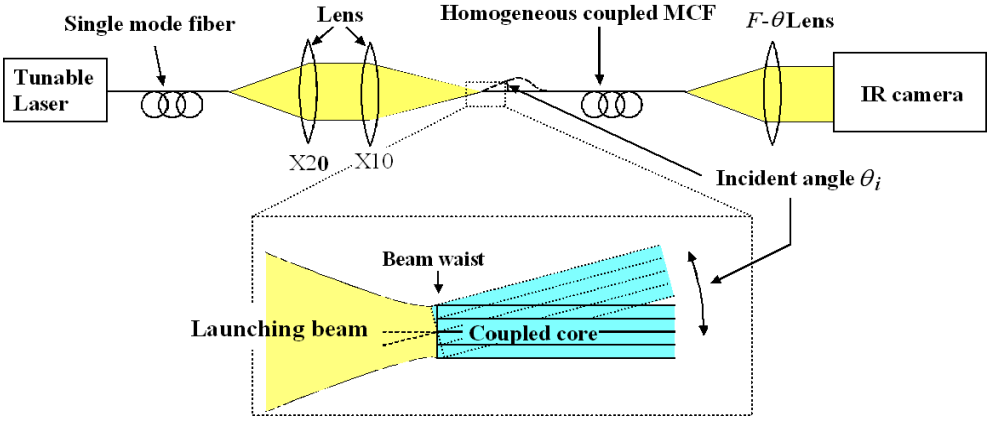


Fig. 4. FFP measurement setup of homogeneous coupled MCF.

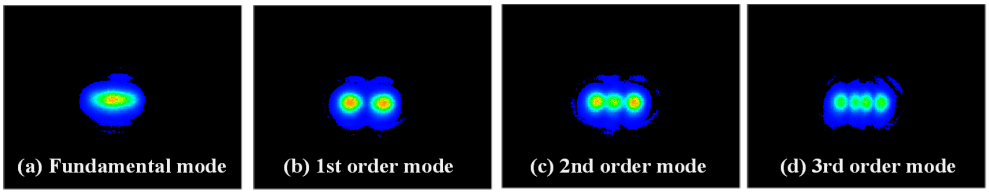


Fig. 5. Measured near-field-patterns of coupled modes.

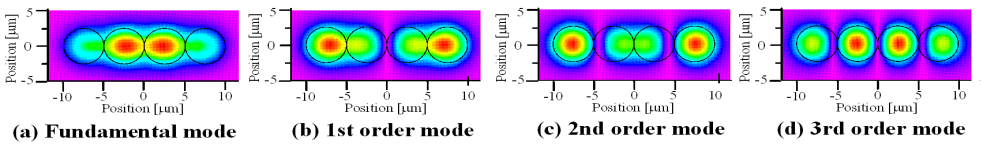


Fig. 6. Calculated near-field-patterns of coupled modes.

#155638 - $15.00 USD Received 29 Sep 2011; revised 21 Nov 2011; accepted 23 Nov 2011; published 8 Dec 2011

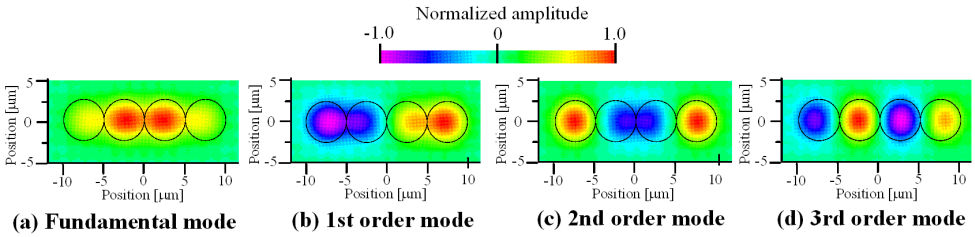


Fig. 7. Calculated field apmplitude patterns of coupled modes.

criminate between the diffraction angles of output beams corresponding to the propagation angle of each coupled mode, we can compare the peak angle of FFP with the incident angle of the launching beam and the calculated results.

We used a far-field observation system consisting of an F-$\theta$ lens and an InGaAs infrared imaging system (C10633-13 and LEPAS-12 by Hamamatsu Photonics Inc.). The angle of incidence of the launching beam was regulated to maximize the peak intensity of FFP of the corresponding mode order.

The measured far-field patterns of coupled modes are shown in Fig. 8 and the calculated FFP's are shown in Fig. 9. It is seen that each coupled mode is selectively excited by changing the incident angle of the launching beam.

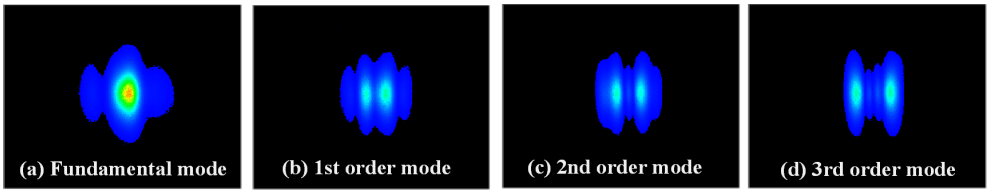


Fig. 8. Measured far-field-patterns of coupled modes.

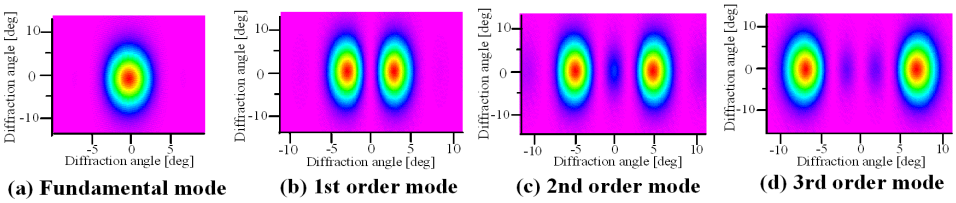


Fig. 9. Calculated far-field-patterns of coupled modes.

## 4. Quantitative evaluation of mode selectivity

Although a strong correlation between the peak angle of FFP and the incident angle of the launching beam, a small variation in FFP was observed when the wavelength of the launching beam was slightly changed (0.04nm) as shown in Fig. 10. The intensity profiles of these FFP's

#155638 - $15.00 USD Received 29 Sep 2011; revised 21 Nov 2011; accepted 23 Nov 2011; published 8 Dec 2011

along the center horizontal axis, which were plotted from the output of LEPAS-12 system, are shown in Fig. 11(a) and (b).

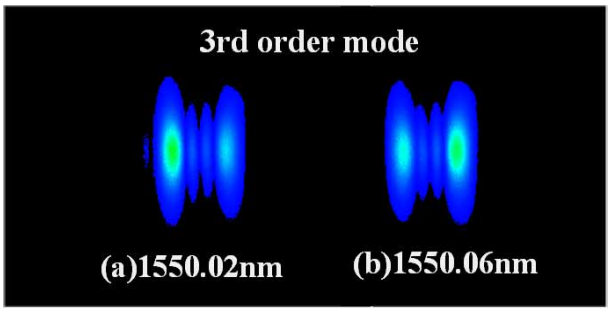


Fig. 10. Variation of FFP of 3rd order mode against small change of wavelength.

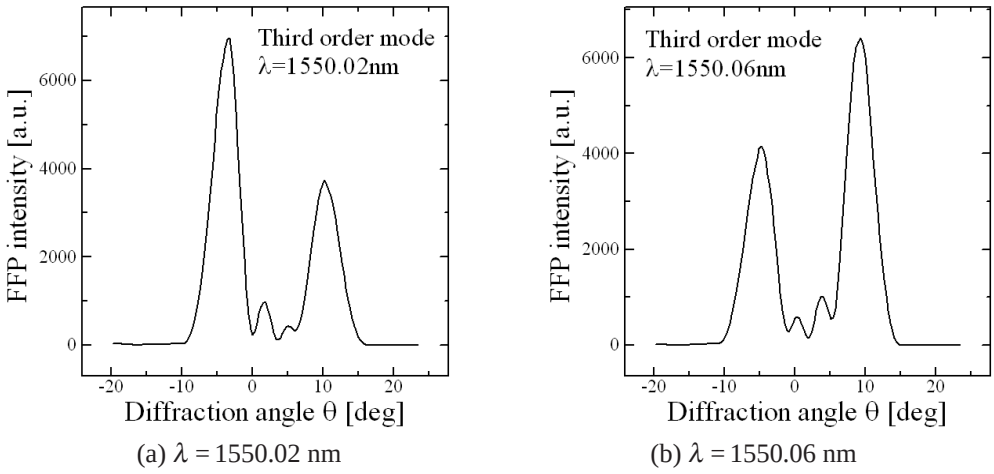


(a) $\lambda$ = 1550.02 nm (b) $\lambda$ = 1550.06 nm

Fig. 11. Intensity profiles of FFP of 3rd order mode against small change of wavelength.

This small change was thought to be caused by the interference between adjacent coupled modes. Although each coupled mode is mostly seletively excited by adjusting the incident angle of the launching beam to the angle corresponding to the propagation angle of the coupled mode, small amount of the adjacent mode may be excited and superimposed on the far-field pattern. Since the parity of the main excited mode and adjacent mode are reversed to each other, the intensity profile of far-field pattern has two unequal peaks, one resulting from the constructive interference and the other resulting from the destructive interference. Therefore, the field amplitude can be calculated from the two far-field patterns, each of which has the maximum peak intensity and the minimum peak intensity in the positive (or negative) diffraction angle region when the wavelength of the launching beam is slightly changed ($\sim$ 0.04 nm).

Now let us define the electric field function of the $\nu$-th order mode in the positive $\theta$ region of FFP by $f_\nu^{(+)}(\theta)$. Then if $\nu$ is an even integer, the whole electric field function can be expressed by

$$f_\nu^{(e)}(\theta) \quad = \quad f_\nu^{(+)}(-\theta) \quad (\theta < 0) \tag{1}$$

#155638 - $15.00 USD Received 29 Sep 2011; revised 21 Nov 2011; accepted 23 Nov 2011; published 8 Dec 2011

$$= \quad f_\nu^{(+)}(\theta) \qquad (0 \le \theta), \tag{2}$$

and if $\nu$ is an odd integer, the whole electric field function can be expressed by

$$f_\nu^{(o)}(\theta) = -f_\nu^{(+)}(-\theta) \quad (\theta < 0) \tag{3}$$

$$= f_\nu^{(+)}(\theta) \qquad (0 \le \theta), \tag{4}$$

because we assumed a symmetric coupled system.

If $\nu$ is assumed to be an odd integer, then ($\nu$-1) is an even integer. When the $\nu$-th order mode and the ($\nu$-1) th order mode are simultaneously excited and the phase relation is the one that the constructive interference occurs in the positive region of diffraction angle of FFP, then the intensity profile of total FFP $|f^{(0)}(\theta)|^2$ is expressed by

$$|f^{(0)}(\theta)|^2 = \left(-f_\nu^{(+)}(-\theta) + f_{\nu-1}^{(+)}(-\theta)\right)^2, \quad (\theta < 0) \tag{5}$$

$$= \left(f_\nu^{(+)}(\theta) + f_{\nu-1}^{(+)}(\theta)\right)^2. \qquad (0 \le \theta) \tag{6}$$

This profile of FFP has two peaks as shown in Fig. 12(a) and the peak in the positive $\theta$ region is greater than that in the negative $\theta$ region owing to the constructive interference. In addition, the position of peak in the positive $\theta$ region is shifted to inner side, because the peak angle of the ($\nu$-1) th order mode is smaller than that of the $\nu$-th order mode. On the other hand, when the phase relation between the $\nu$-th order mode and the ($\nu$-1) th order mode is the one that the destructive interference occurs in the positive region of the diffraction angle of FFP, then the intensity profile of total FFP is expressed by

$$|f^{(\pi)}(\theta)|^2 = \left(-f_\nu^{(+)}(-\theta) - f_{\nu-1}^{(+)}(-\theta)\right)^2, \quad (\theta < 0) \tag{7}$$

$$= \left(f_\nu^{(+)}(\theta) - f_{\nu-1}^{(+)}(\theta)\right)^2. \qquad (0 \le \theta) \tag{8}$$

This profile of FFP has also two peaks as shown in Fig. 12(b), however, the peak in the positive $\theta$ region is smaller than that in the negative $\theta$ region owing to the destructive interference. In addition, the position of the peak in the positive $\theta$ region is shifted to the outer side, because the subtraction of the profiles of the $\nu$-th order mode and the ($\nu$-1) th order mode gives a smaller peak at the outer position than those of the $\nu$-th order mode in the positive $\theta$ region.

The addition and subtraction of Eqs.(6) and (8) give the following simultaneous equations of $|f_\nu^{(+)}(\theta)|^2$ and $|f_{\nu-1}^{(+)}(\theta)|^2$ in the positive region of diffraction angle of FFP.

$$|f^{(0)}(\theta)|^2 + |f^{(\pi)}(\theta)|^2 = 2\left[(f_\nu^{(+)}(\theta))^2 + (f_{\nu-1}^{(+)}(\theta))^2\right] \quad (0 \le \theta) \tag{9}$$

$$|f^{(0)}(\theta)|^2 - |f^{(\pi)}(\theta)|^2 = 4\, f_\nu^{(+)}(\theta)\, f_{\nu-1}^{(+)}(\theta). \qquad (0 \le \theta) \tag{10}$$

Now let us define the left hand side of Eq. (9) and Eq. (10) by $A(\theta)$ and $B(\theta)$, respectively. Then the solutions of the above simultaneous equations are given by

$$\left(f_\nu^{(+)}(\theta)\right)^2 = \frac{A(\theta) + \sqrt{A(\theta)^2 - B(\theta)^2}}{4} \quad (0 \le \theta) \tag{11}$$

$$\left(f_{\nu-1}^{(+)}(\theta)\right)^2 = \frac{A(\theta) - \sqrt{A(\theta)^2 - B(\theta)^2}}{4} \quad (0 \le \theta) \tag{12}$$

Therefore, by measuring the FFP's $|f_\nu^{(0)}(\theta)|^2$ and $|f_\nu^{(\pi)}(\theta)|^2$ which give the maximum and minimum peaks when the wavelength is slightly changed, the FFP $\left(f_\nu^{(+)}(\theta)\right)^2$ of the $\nu$-th

#155638 - $15.00 USD Received 29 Sep 2011; revised 21 Nov 2011; accepted 23 Nov 2011; published 8 Dec 2011

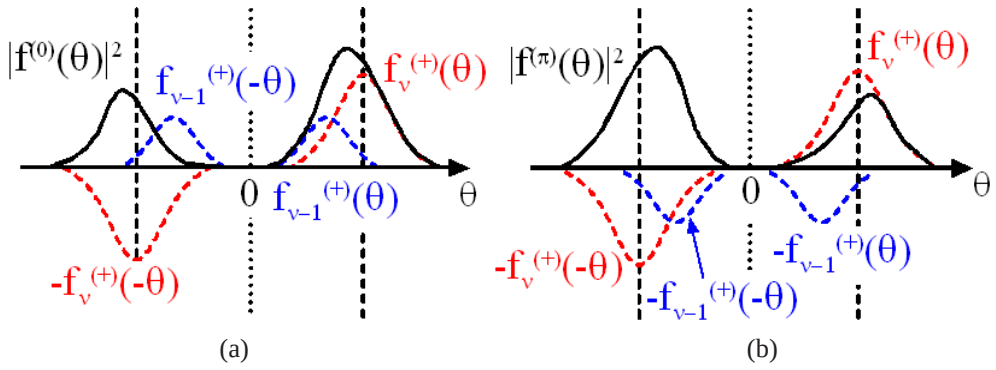


Fig. 12. Phase relation of FFP of even and odd coupled modes and the total FFP intensity. (a) constructive interference in positive $\theta$ (b) destructive interference in positive $\theta$

order mode and the $\left(f_{\nu-1}^{(+)}(\theta)\right)^2$ of the $(\nu-1)$-th order mode can be separately obtained from Eqs.(11) and (12).

In the measured far-field pattern, the profile is not always symmetric with respect to the center axis, and so we calculated the FFP's of adjacent modes by separating the FFP into the positive and negative diffraction angle regions.

Since the above mode discrimination method assumed that only two coupled modes exist and interefere with each other, we discriminated the fundamental mode and the 1st order mode when the incident angle of the launching beam was 0 degree, and also the 2nd order mode and the 3rd order mode when the incident angle of the launching beam was 6.6 degrees which maximized the FFP of the 3rd order mode. The discriminated FFP's are shown in Fig. 13(a) and (b).

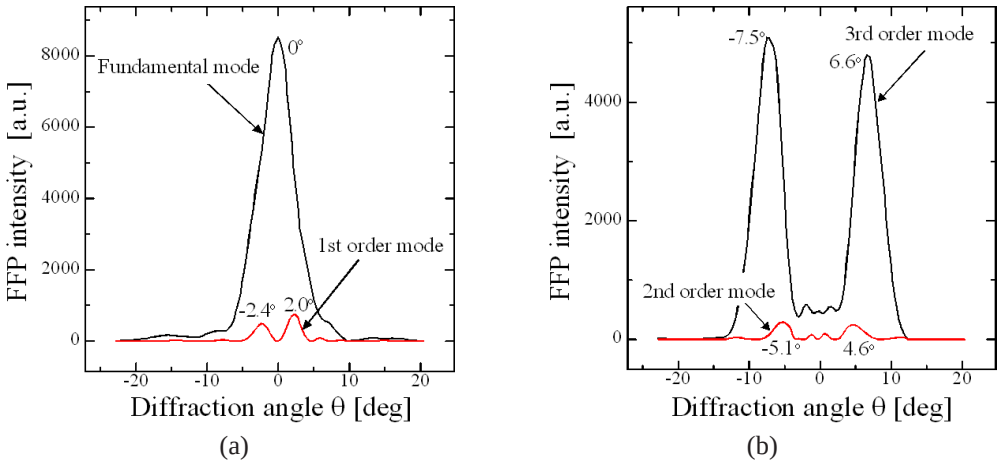


Fig. 13. Discriminated far-field patterns from the visibility measurement of FFP. (a) fundamental mode excitation (b) 3rd order mode excitation

From these measurements, the extinction ratio (mode selectivity of excitation) for the case of fundamental mode excitation was evaluated to be -11 dB (excitation of the 1st order mode),

#155638 - $15.00 USD Received 29 Sep 2011; revised 21 Nov 2011; accepted 23 Nov 2011; published 8 Dec 2011

and that for the 3rd order mode excitation was -13 dB (excitation of the 2nd order mode). The peak angles of discriminated FFP of output beam from the homogeneous MCF are summarized in Table 2, comparing with the incident angle of the launching beam and the theoretical value. The peak angles show a strong correlation with the incident angle of the launching beam, which means that the coupled modes were almost selectively excited and discriminated.

Table 2. Comparison of incident angle, peak angle of FFP, and the theoretical value.

| | Angle of incidence of launching beam | Discriminated peak angle of FFP | Theoretical peak angle of FFP |
|---|---|---|---|
| 0th order mode | 0 | 0 | 0 |
| 1st order mode | 2.73 | 2.20 ($\pm$0.20) | 3.0 |
| 2nd order mode | 4.07 | 4.89 ($\pm$0.22) | 5.0 |
| 3rd order mode | 6.62 | 7.05 ($\pm$0.45) | 7.4 |

*Unit of all angles is [degrees].

## 5. Conclusion

We successfully demonstrated the selective excitation of coupled modes in a homongeneous coupled multi-core fiber for the first time. The FFP profiles of coupled modes were discriminated quantitatively from the visibility measurement of FFP when the wavelength was slightly changed. The extinction ratio (mode selectivity of excitation) between the fundamental and the 1st order modes was evaluated to be -11 dB for the fundamental mode excitation, and that between the 3rd and the 2nd order modes was -13 dB for the 3rd order mode excitation. This mode discrimination technique will be usefull to the quantitative investigation of the crosstalk and the bending properties of homogeneous coupled multi-core fibers, and the experimental results measured by this technique will be presented in future.

## Acknowledgements

This research is supported by the National Institute of Information and Communications Technology(NICT), Japan under “Research on Innovative Optical Fiber Technology.”

#155638 - $15.00 USD Received 29 Sep 2011; revised 21 Nov 2011; accepted 23 Nov 2011; published 8 Dec 2011